Addressing optimal underwater electrical explosion of a wire

A. Virozub, V. Tz. Gurovich, D. Yanuka, O. Antonov, and Ya. E. Krasik
Physics Department, Technion, Haifa 32000, Israel

(Received 24 May 2016; accepted 6 September 2016; published online 22 September 2016)

The underwater electrical explosion of a wire in the timescale 10^{-7}–10^{-6} s is characterized by different phase transitions at extreme values of deposited energy density, allowing one to obtain warm dense matter using rather moderate pulse power generators. In order to achieve maximal energy density deposition, the parameters of the wire and the pulse generator should be optimized to realize an overdamped explosion where most of the initially stored energy is delivered to the exploding wire during a time comparable with the quarter of the discharge period. In this paper, the results of 1D magneto-hydrodynamic modeling, coupled with the copper and water equations of state, of the underwater electrical explosion of Cu wires having an identical length and average current density but different discharge current rise time are analyzed and compared with those of a simplified model of a conductivity wave, the propagation velocity of which determines the mode of the wire's explosion. In addition, it is shown that in the case of extreme high current densities, a scaling from a single wire to a wire array having the same total cross-sectional area of wires cannot be used to obtain an optimal wire explosion. *Published by AIP Publishing.*
[http://dx.doi.org/10.1063/1.4963002]

I. INTRODUCTION

The underwater electrical explosion of a wire allows one to achieve an extremely high energy density deposition (>200 eV/atom) during $\leq 10^{-6}$ s.[1] Such high energy density deposition becomes available because of the low compressibility of water, resulting in a rather slow wire radial expansion velocity $\sim 10^5$ cm/s, and because of the high value of the breakdown electric field in water (~300 kV/cm), preventing the formation of a shunting plasma channel along the wire's surface, typical for wire explosions in vacuum or gas.

In order to achieve high energy density deposition, a wire explosion characterized by an overdamped discharge, i.e., when the damping parameter $\varsigma = 0.5R\sqrt{C/L} \geq 1$, should be realized. Here, $R(t)$ is the time-dependent resistance of the exploding wire and C and $L(t)$ are the capacitance and inductance of the discharge circuit, respectively. In this case, a significant (>60%) part of the energy primarily stored in the capacitor bank is transferred to the exploding wire during a time shorter than the discharge's half of a period. To obtain an overdamped discharge, one can apply a simplified model of the wire's explosion and use similarity parameters[2] to define the parameters of the electrical circuit, namely, capacitance, inductance, and charging voltage, as well as the parameters of the wire, i.e., radius, length, and material. This model considers uniform wire evaporation and conductivity of the wire proportional to the deposited energy density. However, wire electrical explosion is a rather complicated phenomenon, characterized by phase transitions (solid state–liquid–vapor–plasma) and radial expansion of the wire due to pressure gradients. These processes lead to fast changes in the wire's electrical and thermal conductivities, density, pressure, and temperature, which cannot be considered to be independent of each other. In recent years, a self-consistent magneto-hydrodynamic (MHD) modeling, coupled with Ohm's law, electrical circuit equations, equations of state (EOS), and electrical conductivity models of an underwater wire explosion was conducted in a broad range of wire and current pulse parameters.[3] This modeling allows one to obtain the resistive voltage and discharge current waveforms in the *RLC* circuit (here R is the total resistance of the discharge circuit) and, consequently, the energy density deposition into the wire for a known charging voltage of the capacitor bank. In experiments with Cu wire underwater electrical explosions, the wire's resistance was changed from its resistance of $\sim 10^{-2}$ Ω to several Ohms during 10^{-7}–10^{-6} s, depending on the pulse generator's parameters.

In the case of an optimal wire explosion characterized by an overdamped mode of the electrical discharge, the discharge current reaches its maximal amplitude of $\sim 0.8 I_{sc}$, where I_{sc} is the amplitude of the current in the case of a pure inductive load.[1] During this rise time of the current, the wire experiences fast Joule heating accompanied by solid state-liquid and partial liquid-vapor phase transitions characterized by a significant increase in the wire's total resistance. Typically, in the case of an optimal wire explosion, ~30% of the initially stored energy W_0 in the capacitor banks is deposited into the wire during this discharge phase. Later in the discharge, a much faster increase in the wire's resistance is realized, leading to a fast decrease in the discharge current and generation of voltage along the exploding wire $\varepsilon = I(t)R_w(t) + L_w(t)\,dI(t)/dt + I(t)dL_w(t)/dt$, where $L_w(t)$ is the time-dependent inductance of the wire due to its radial expansion and $I(t)$ is the discharge current. During this phase of the discharge, a low-ionized, non-ideal plasma is formed as a result of partial ionization of the wire vapors. The wire's maximal resistance is realized close to the peak of the generated voltage, and later in the discharge one obtains a decrease in the wire's resistance. However, this decrease in the resistance should not be sufficient to transfer the discharge into an under-damped mode.

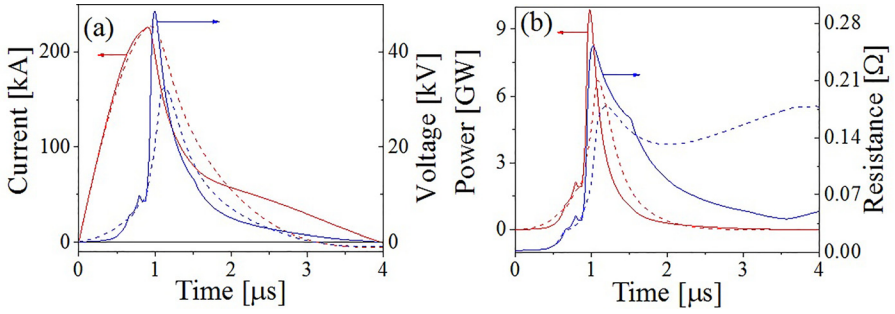

FIG. 1. (a) Waveforms of the discharge current and resistive voltage; (b) temporal evolution of the deposited power and resistance. Solid line: Cu wire array: 40 wires 40 mm in length and 100 μm in diameter. Dashed line: Cu wire 632 μm in diameter and 40 mm in length.

The wire's cross section S, necessary to obtain an electrical explosion at $\sim 0.8 I_{sc}$, can be estimated using the action integral g as $S^2 = g^{-1} \int_0^{t_{exp}} I^2(t)dt$ having tabulated data for different metals.[4] Considering this value of S and $\sim 0.3 W_0$ energy deposited into the wire to achieve its evaporation within the time interval of t_{exp}, one can estimate the wire's length. These calculations do not account for a fast change in the wire's resistance during the heating and evaporation of the wire and can be considered only as rough estimates of the wire and electrical circuit parameters necessary to obtain an optimal wire explosion.

II. MHD MODELING OF DIFFERENT WIRES UNDERWATER ELECTRICAL EXPLOSION

MHD modeling shows that, for the same average current density, electrical explosions of a single wire with a cross-sectional area S_0 and an array of wires having the same length and total cross section as the single wire result in different time-dependent resistances and, consequently, energy density depositions. Let us consider the underwater electrical explosions of a 10 mm in diameter array of 40 Cu wires each of which is 40 mm in length and 100 μm in diameter with a return current path having a diameter of 80 mm, and of a single Cu wire having the same length but a 632 μm diameter, so that it has the same cross-sectional area as the array wires. The pulse generator has a capacitor $C = 10$ μF charged up to 28 kV, total inductance of $\sim$75 nH, and load inductance of $\sim$39 nH. Here, for simplicity the inductances of the single wire and the array of wires are considered to be equal. The 1D MHD modeling was the same as that explained in detail in Ref. 5; the SESAME EOS[6] was used for copper and water and the BKL[7,8] model was applied for electrical conductivity calculations. The waveforms of the discharge current and resistive voltage and temporal evolution of the deposited power and resistance (the latter is calculated based on spatial integration of the data of the conductivity's radial distribution and assuming axial and azimuthal uniformities) for the single wire and the wire array are shown in Figs. 1(a) and 1(b). One can see that, despite the fact that the maximal amplitude of the discharge current in both cases is almost the same, the rate of the current decrease, dI/dt, and, consequently, the amplitude of the resistive component of the voltage ($\sim$48 kV), maximal deposited power (10 GW), and maximal resistance (0.25 Ω) are significantly larger for the wire array than for the single 632 μm diameter wire. Here, let us note that the resistance of a single 100 μm diameter wire in the array reaches $\sim$10 Ω.

To understand the differences in the deposited power during these explosions, let us analyze the parameters of the wires that are realized at different discharge times. In Table I, the average radial values of expansion velocity, density, and radii of the thin (i.e., a single wire of the wire array) and thick (632 μm in diameter) wires at the maximal amplitude of the discharge current, resistive voltage, and resistance are presented. Here, n_0 is the density of Cu at normal conditions. One can see that the average expansion velocity of the thin wire is smaller, but the decrease in density is larger than that obtained for the thick wire.

The radial distributions of temperature and conductivity that are realized at the maximal amplitude of the discharge current for these two cases are shown in Fig. 2. Here, for the case of the wire array, these distributions are plotted for a single thin wire. At this time, the wires are expanded to radii of $\sim$75 μm and $\sim$420 μm, which correspond to the average radial expansion velocity of $\sim 2.8 \times 10^3$ cm/s and $\sim 10^4$ cm/s, respectively. In addition, one can see that in both cases, there is a sharp decrease in the temperature at the periphery of the wires related to their cooling by water within $\sim$10 μm and $\sim$45 μm for the thin and thick wires, respectively. However,

TABLE I. Average radial values of expansion velocity and density and radii of a single wire in the wire array and a thick (632 μm in diameter) wire at maximal amplitude of the discharge current, resistive voltage, and resistance.

Maximum current				Maximum voltage				Maximum resistance			
Cu wire		Cu wire		Cu wire		Cu wire		Cu wire		Cu wire	
$r_0 = 50$ μm		$r_0 = 316$ μm		$r_0 = 50$ μm		$r_0 = 316$ μm		$r_0 = 50$ μm		$r_0 = 316$ μm	
227 kA		230 kA		48 kV		33 kV		0.25 Ω		0.18 Ω	
$t_1 = 900$ ns		$t_1 = 940$ ns		$t_2 = 1000$ ns		$t_2 = 1120$ ns		$t_3 = 1020$ ns		$t_3 = 1190$ ns	
$r = 75$ μm		$r = 420$ μm		$r = 150$ μm		$r = 630$ μm		$r = 177$ μm		$r = 750$ μm	
V_{av} 10^5 cm/s	n/n_0	V_{av} 10^5 cm/s	n/n_0	V_{av} 10^5 cm/s	n/n_0	V_{av} 10^5 cm/s	n/n_0	V_{av} 10^5 cm/s	n/n_0	V_{av} 10^5 cm/s	n/n_0
0.028	0.44	0.11	0.57	0.75	0.11	1.17	0.26	1.35	0.08	1.71	0.18

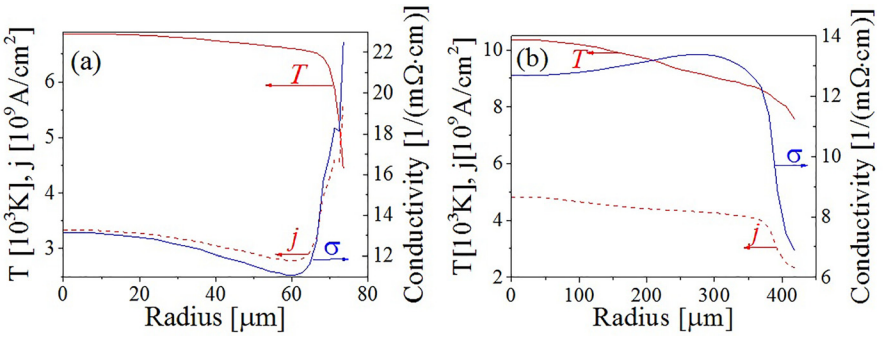

FIG. 2. Radial distributions of temperature, conductivity, and current density at the time of maximal amplitude of the discharge current (a) in the case of a thin, 100 μm diameter wire ($t_1 = 900$ ns) and (b) a thick, 632 μm diameter wire ($t_1 = 940$ ns). Solid lines: temperature and conductivity. Dashed lines: current density.

if in the case of the thin wire this cooling (from 6500 K down to 4400 K) leads to an increase in its conductivity and current density at that location, in the case of the thick wire, one obtains the opposite dependence, i.e., a decrease in the temperature from 8500 K to 7600 K, which leads to an almost two-fold decrease in conductivity and current density. In the core of the wires, the temperature increases insignificantly toward the axis, but the value of the temperature is ~20% larger in the case of a thick wire, reaching ~10 300 K at the axis of the wire. In addition, one can see that, in the core of the wires, the conductivity is almost the same, but the current density is smaller in the case of the thin wire. In the case of a low-ionized and low-temperature ($\leq$10 300 K) plasma, the conductivity is proportional to $\sigma \propto n_e/T_e^{1/2}\sigma_{tr}n_a$, where n_e and T_e are the density and temperature of electrons, σ_{tr} is the transport electron collision cross section, and n_a is the density of neutral atoms $n_a \propto [1 + (V_{\exp}t/r_0)]^{-2}$, where $V_{\exp}$ is the expansion velocity of the wire, t is the time, and r_0 is the initial wire radius. Thus, one can see that dependence $\sigma = f(T_e)$ is rather complicated because of the dependence of the electrons and atoms' densities on temperature and time.

In Fig. 3, the same radial distributions of the wire parameters are shown at the time of maximal amplitude of the resistive voltage. At that time, the thin and thick wires are expanded to radii ~150 μm and ~610 μm, respectively, which correspond to an average expansion velocity of $\sim 0.75 \times 10^5$ cm/s and $\sim 1.17 \times 10^5$ cm/s, respectively, within the time interval between the maxima of the current and voltage. During this phase, the temperature of the thick wire gradually increases up to ~19 000 K at the axis. Further, in the case of the thick wire, one obtains an almost linear increase in the conductivity and current density toward the axis. However, in the case of the thin wire a rather non-uniform, wave-like radial distribution of the parameters was obtained. In the core of the thin wire at $r < 110$ μm, the decrease/increase in temperature is followed by a decrease/increase in the conductivity and current density. However, at the larger radii, the decrease in temperature is accompanied by an increase in conductivity and, correspondingly, in current density. In addition, similar to the time of the maximal current amplitude, at this time the temperature and conductivity of the thick wire are ~1.5 and ~4.5 larger than that in the case of a thin wire explosion, respectively.

During the next tens of nanoseconds when the maximum resistance is obtained, the average radial expansion velocity increases to $\sim 1.35 \times 10^5$ cm/s and $\sim 1.71 \times 10^5$ cm/s for the thin and thick wires, respectively. In this short time interval (see Fig. 4), one obtains an increase in temperature of up to ~14 500 K and ~21 000 K for the thin and thick wires, respectively, and opposite radial dependencies of the conductivities. Namely, in the case of the thin wire, the conductivity increases step-wise toward the periphery, and in the case of the thick wire, the conductivity increases toward the axis.

Thus, the results of this modeling showed that, although the amplitude and rise time of the discharge current and average current density are the same for an array of wires having the same total cross-sectional area as a single thick wire, the parameters of the electrical explosion can be significantly different. So, a simple scaling from a single wire to a wire array having the same total cross-sectional area of wires cannot be used to obtain an optimal electrical explosion.

Next, another comparison was performed, where the results of one-dimensional MHD modeling of the underwater electrical explosion of single thick Cu wires (initial resistance is ~2.17 mΩ) with the same length, $l = 45$ mm, radius, $r_0 = 0.316$ mm, and amplitude of the discharge current but with a different rise time of the current pulse were considered. In the first case, the wire explosion is realized by the

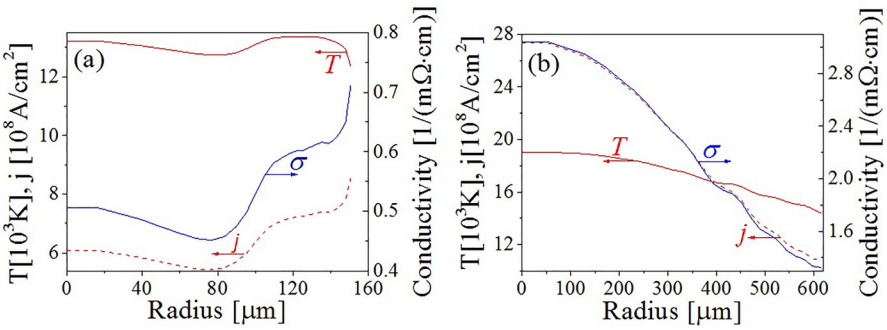

FIG. 3. Radial distributions of temperature, conductivity (solid lines), and current density (dashed lines) at the time corresponding to the maximum of the resistive voltage in the case of (a) a thin 100 μm diameter wire ($t_2 = 1000$ ns) and (b) a thick 632 μm diameter wire ($t_2 = 1120$ ns). Solid lines: temperature and conductivity. Dashed lines: current density.

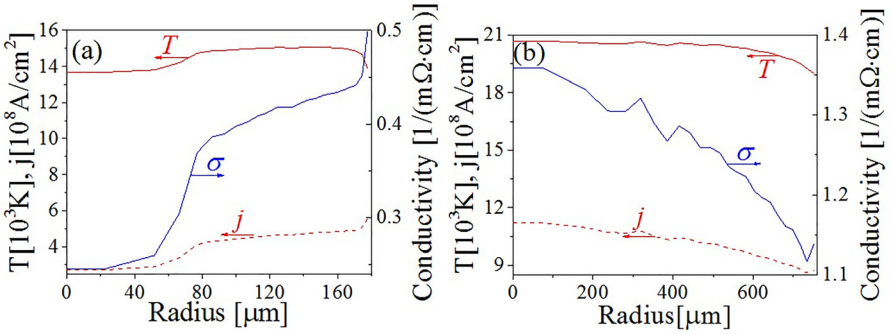

FIG. 4. Radial distributions of the temperature, conductivity (solid lines), and current density (dashed lines) at the time corresponding to the maximum of the resistance in the case of (a) a thin 100 μm diameter wire ($t_3 = 1020$ ns) and (b) a thick 632 μm diameter wire ($t_3 = 1190$ ns). Solid lines: temperature and conductivity. Dashed lines: current density.

discharge of a capacitor bank with a capacitance of $C = 10\,\mu$F and charged to a voltage of $U \approx 28$ kV(this case was considered in previous analyses of the single thick wire and wire array), and in the second case, the capacitance was decreased to $C = 1\,\mu$F, while the charging voltage was increased to $U \approx 88.5$ kV. These changes in capacitance and charging voltage allow one to obtain the same amount of stored energy ($\sim$3.92 kJ) and the same amplitude of the discharge current but with a different rise time in the case of an identical inductive load. In the first case with a short-circuit inductive load, the amplitude of the current is $I_m \cong 300$ kA with quarter of a period $T/4 \cong 1.34\,\mu$s and an average current density across the wire's cross-section $j_{av} \cong 10^8$A/cm^2. Hereafter, this case is designated a "long" explosion. In the second case, one obtains the same amplitude of the discharge current and its averaged current density, but with quarter of a period of $\sim$0.4 μs. Hereafter, this wire explosion is designated a "short" explosion. The waveforms of the discharge current and resistive voltage and deposited power and energy for the "long" and "short" wire electrical explosions are shown in Figs. 5 and 6.

One can see that the "long" wire explosion is characterized by an aperiodic discharge, with the current reaching its maximal amplitude of $\sim$230 kA within $\sim$0.93 μs (see Fig. 5(a)). Further, one obtains a fast decrease in the discharge current. During this phase, the duration of which is $\sim$420 ns, one obtains a resistive voltage with an amplitude up to 37 kV, delivering the main part of the stored energy (up to 3.1 kJ) to the exploding wire, with power reaching $\sim$7.85 GW (see Fig. 6(a)). This phase, which can be designated the wire explosion phase, is characterized by a fast increase in the wire's resistance (calculated by spatial integration of the conductivity's radial distribution obtained as the result of the MHD simulation) up to $\sim$0.18 Ω (see Fig. 7(a)) within a time interval 0.83–1.2 μs, followed by a slow (within $\sim$1 μs) decrease in the resistance to $\sim$0.15 Ω. At that time, $\sim$95% of the stored energy has been deposited into the wire. Let us consider this case as an optimal wire explosion.

Significantly different parameters of the wire's explosion are obtained in the case of a "short" wire explosion characterized by a periodical discharge (see Fig. 5(b)). One can see that, despite the current reaching a larger amplitude of $\sim$290 kA within $\sim$410 ns, the resistive voltage does not exceed 33 kV and has a long ($\sim$600 ns) rise time. Correspondingly, the energy delivered to the wire does not exceed 2.4 kJ during half of the discharge period and the maximal power is lower than 7.25 GW (see Fig. 6(b)). Further, the resistance of the wire increases significantly more slowly, remaining <0.2 Ω during the first 700 ns of the wire's explosion (see Fig. 7(b)).

In Figs. 8–11, the radial distributions of the temperature, current density, and normalized conductivity σ/n and n/n_0 are shown for different times of the wire explosions for these two cases. Here n_0 and n are the density of copper at normal conditions and during the wire explosion, respectively. During the rise time of the discharge current (see Fig. 8), one already obtains a large difference in the radial distributions of temperature due to different timescales of the current's penetration toward the axis. Namely, if in the case of the "long" explosion, at $t = 510$ ns, the temperature increases to 400 K at $r = 95\,\mu$m because of Joule heating, and the same temperature is realized at $r = 155\,\mu$m in the case of the "short" explosion. The latter leads to different conductivity and current density radial distributions, resulting in a higher temperature at the wire's periphery for the "short" explosion.

At the maximum amplitude of the discharge current, this difference in temperature distributions increases (see Fig. 9). For the case of the "long" explosion, the temperature gradually increases toward the axis, reaching almost 11 000 K, and in the case of the "short" explosion, the maximum temperature of $\sim$8000 K is obtained at $r = 235\,\mu$m with a fast decrease

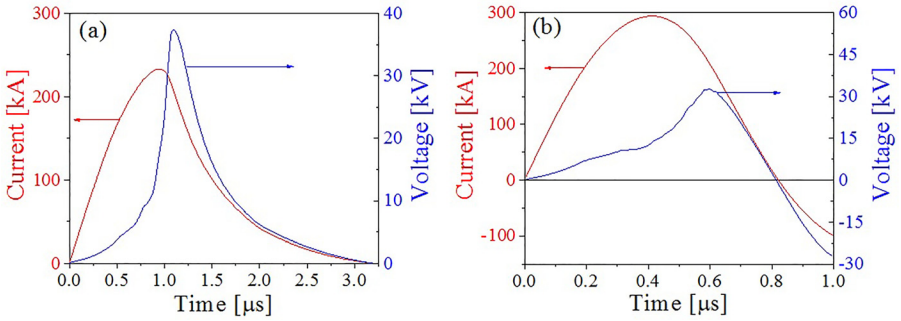

FIG. 5. Waveforms of the discharge current and resistive voltage for Cu wire underwater electrical explosion. (a) $C = 10\,\mu$F and $U = 28$ kV and (b) $C = 1\,\mu$F and $U = 88.5$ kV.

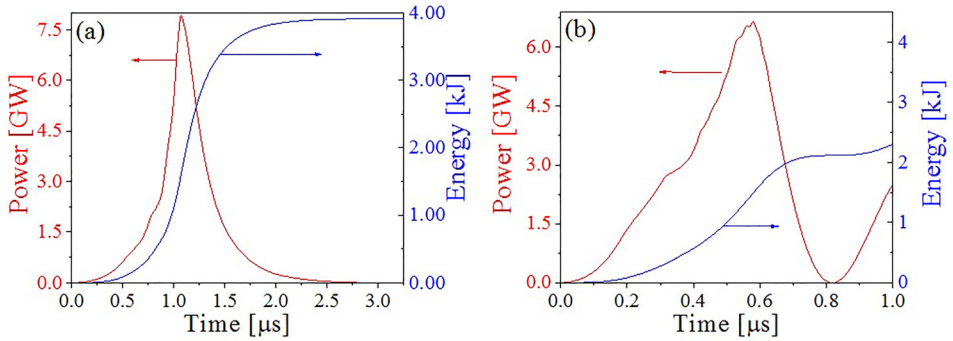

FIG. 6. Deposited power and energy for Cu wire underwater electrical explosion. (a) $C = 10\,\mu$F and $U = 28$ kV and (b) $C = 1\,\mu$F and $U = 88.5$ kV.

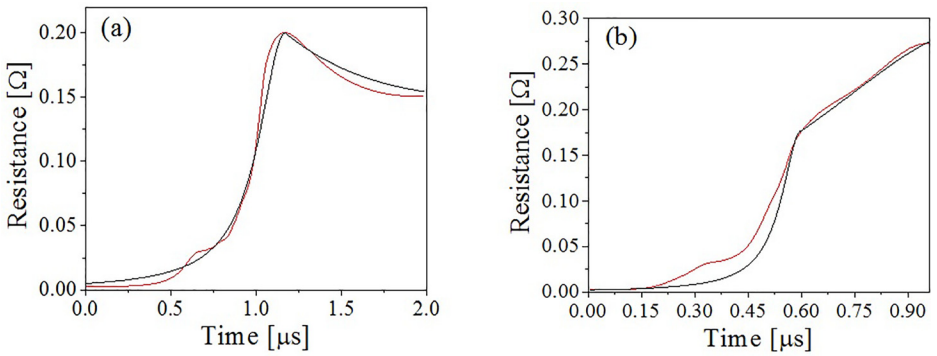

FIG. 7. Time dependence of the exploding wire's resistance obtained by MHD simulations (red) and from simplified resistance model (black). (a) $C = 10\,\mu$F and $U = 28$ kV and (b) $C = 1\,\mu$F and $U = 88.5$ kV.

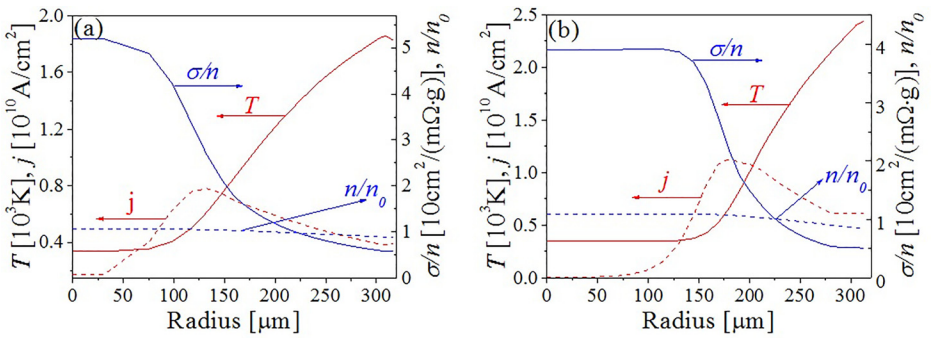

FIG. 8. Radial distributions of temperature, current density, and normalized conductivity and density, and for "long" (a) and "short" (b) wire explosions obtained for "long" explosions at $t = 510$ ns and for "short" explosions at $t = 209$ ns.

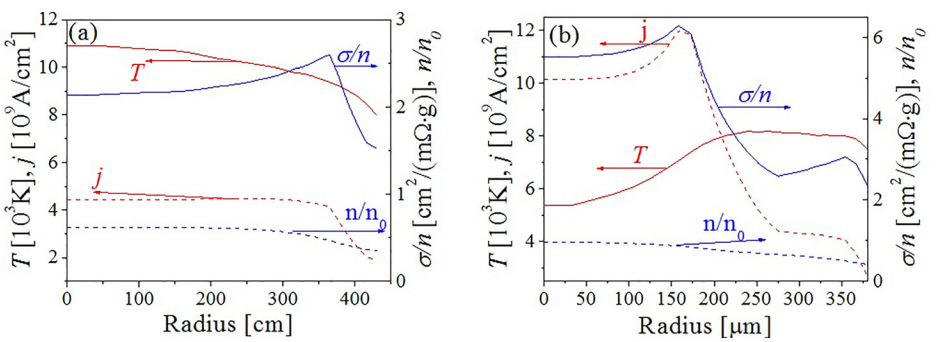

FIG. 9. Radial distributions of temperature, conductivity, current density, and normalized conductivity and density for "long" (a) and "short" (b) wire explosions obtained for "long" explosions at $t = 930$ ns and for "short" explosions at $t = 419$ ns. These times correspond to the maximal current amplitude.

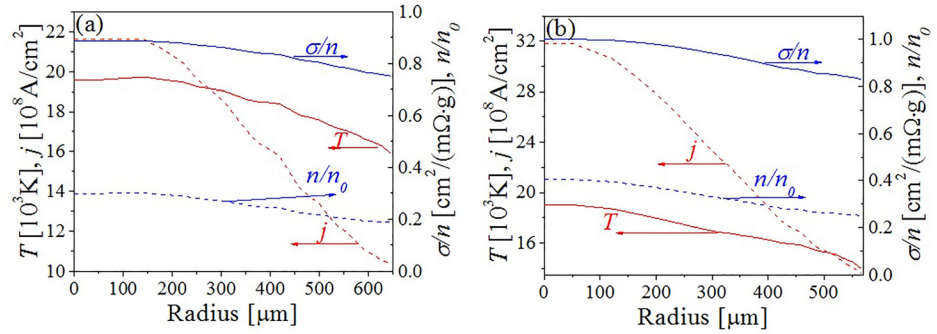

FIG. 10. Radial distributions of temperature, conductivity, current density, and normalized conductivity and density for "long" (a) and "short" (b) wire explosions obtained at $t = 1110$ ns for "long" explosions and at $t = 600$ ns for "short" explosions. These times correspond to the maximal voltage amplitude.

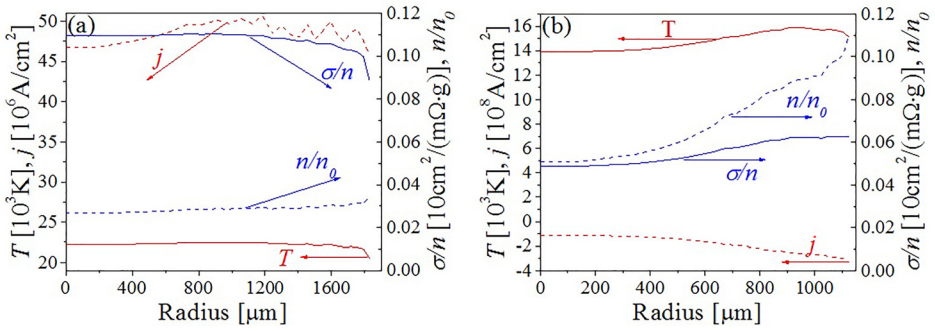

FIG. 11. Radial distributions of temperature, conductivity, current density, and normalized conductivity and density for "long" (a) and "short" (b) wire explosions obtained at $t = 1982$ ns for "long" explosions, and at $t = 960$ ns for "short" explosions.

toward the axis. Further, one can see that the conductivity and current density are almost uniform at $r \leq 360\ \mu$m in the case of the "long" explosion. In this case, considered as an optimal wire explosion, the temperature's radial distribution is also almost uniform at $r \leq 360\ \mu$m. In the case of the "short" explosion, these distributions are highly non-uniform, characterized by almost normal Cu conductivity at $r < 150\ \mu$m and a fast decrease in the current density at $r > 150\ \mu$m. At that time, in the case of the "long" explosion, because of radial expansion, the wire's radius increases to 420 μm and increases only to ~375 μm in the case of the "short" wire explosion.

At the time of the maximum amplitude of the resistive voltage, one obtains qualitatively similar radial distributions of the wire parameters. However, if in the case of the "long" explosion at $r < 150\ \mu$m, the temperature and current density reach ~18 600 K and $\sim 2.17 \times 10^9$ A/cm^2, respectively, in the case of the "short" explosion the temperature and current density are ~19 000 K and $\leq 3.2 \times 10^9$ A/cm^2, respectively. Such relatively small current density is related to the dissipation of a significant part of the energy into the wire from the time of the beginning of the discharge current. In addition, let us note the significantly larger radial expansion of the wire in the case of the "long" explosion ($r \cong 630\ \mu$m) than in the case of the "short" explosion ($r \cong 570\ \mu$m), resulting in greater density of the wire in the second case.

Fast radial wire expansion occurs approximately after the time when one obtains the maximum in the resistive voltage (see Figs. 10 and 11). Indeed, at this time period, the discharge current decreases considerably leading to fast decreasing of the magnetic pressure, and due to large internal pressure, one obtains fast radial wire expansion with a velocity of up to ~$2 \cdot 10^5$ cm/s. In the case of a "long" explosion, the wire expansion becomes dominant in the process of the wire's resistance evolution, and in spite of a continuing decrease of the conductivity, the resistivity also decreases. In the case of the "short" explosion, the wire's expansion is not sufficient to compensate for the decrease of conductivity, so the resistance continues to increase.

Thus, one can see that in both cases [(a) identical cross section area of a single wire and an array of wires with the same length and total cross section as the single wire and amplitude and rise time of the discharge current; (b) identical wires with the same amplitude of the discharge current but different rise times of the current] one obtains rather different parameters of the exploding wires and different energy density depositions are realized. To explain these differences in the electrical explosion of the wires, a simplified model based on the propagation of a conductivity wave toward the axis of the wire is now considered.

III. SIMPLIFIED CONDUCTIVITY WAVE MODEL

First let us note that the results of MHD modeling showed that the initial heating of the conductor begins at the periphery of its cross sections (skin effect), where the main source of Joule heating with a current density of j^2/σ is located. Later in the discharge, depending on the amplitude of the current density, one obtains a diffusion of the current and, consequently, self-magnetic field penetration toward the axis of the wire. Together with this diffusion, also the heat source and consequently the heated region with the decreased specific conductivity are moving toward the conductor's axis, while the remaining non-heated inner region of the wire has higher conductivity.

Let us consider the propagation of a wave with decreased conductivity and constant front velocity $w = \text{const}$ from the wire periphery toward the axis in a Lagrangian coordinate r. Behind the front of this wave, the conductor has constant conductivity $\sigma \ll \sigma_0$, where σ_0 is the initial conductivity of copper. In Lagrangian coordinates, the wire's radius r_0 remains constant. In this case, the effective conductivity in the expression for the total wire resistance, $R \approx l/\pi\sigma_{eff} r_0^2$, should be expressed as $\sigma_{eff} = \sigma[r(t)/r_0]^2$. At time t, the radius of the non-heated cylindrical volume is $r(t) = r_0 - wt$ and the total resistance of the wire can be calculated as

$$R(t) = R_0/[(1 - Wt)^2 + \beta W t(2 - Wt)];$$
$$R_0 = l/\pi r_0^2 \sigma_0; \quad \beta = (\sigma_{eff}/\sigma_0); \quad W = w/r_0. \qquad (1)$$

Equation (1) describes the resistance dynamics starting from $t = 0$. At time $t_3 = 1/W$, the conductivity wave approaches the axis. At that time, the wire's resistance reaches its extremum (maximal) value

$$[(dR(t)/dt)_{t_3}] = 0 \qquad (2)$$

with

$$R(t_3) = R_0/\beta. \qquad (3)$$

This model has two non-known parameters, β and W, the values of which can be found using numerically obtained values of the resistance $R(t)$, namely, W, t_3, and $R(t_3)$—from the maximum condition (2), β—from Equation (3).

Let us note that at $t \approx t_3$ one obtains a fast radial expansion of the wire (see Table I). The resistance dynamics starting from $t > t_3$ is described by a second conductivity wave. In this description, the same Equation (1) can be used with t replaced by $t - t_3$, and R_0–by $R(t_3)$

$$R(t) = \frac{R_{\max t=3}}{\left(1 - \frac{t - t_3}{t_4 - t_3}\right)^2 + \left(\frac{R_{\max t_3}}{R_{\min x t_4}}\right)\left(\frac{t - t_3}{t_4 - t_3}\right)\left(2 - \frac{t - t_3}{t_4 - t_3}\right)}, \quad t_3 \le t \le t_4. \tag{4}$$

This modified equation is used for describing the second conductivity wave. The new values of W and β are determined from the next extremal value of R at $t = t_4$

$$W = 1/(t_4 - t_3), \tag{5}$$

$$R(t_4) = \frac{R(t_3)}{\beta}. \tag{6}$$

Plots of the resistance dynamics corresponding to the simplified model depicted in Fig. 7 describe the first ($t < t_3$) and the second ($t_4 > t > t_3$) conductivity waves. For the "long" explosion $\beta > 1$, and R decreases at $t > t_3$, while for the "short" explosion $\beta < 1$ and R continues to increase. That is the reason one obtains a breakpoint at $t = t_3$ in the model resistance plot Fig. 7(b).

At $t > t_3$, the wire's conductivity does not change significantly, but its radial expansion leads to a decrease in the wire's total resistance in the "long" explosion case. This can be modeled as a new conductivity wave propagating from the wire periphery. A comparison of the resistance of the wire obtained by this simplified model with the resistance obtained by MHD modeling (see Fig. 7(a)) shows good agreement.

In the case of the "short" wire explosion (see Figs. 8(b)–10(b)), at the beginning of the discharge, when the current does not reach its maximal value, the largest current density is realized at the periphery of the wire. Similar to the case of the "long" wire explosion, the thermal wave propagation toward the axis of the wire is accompanied by a decrease in the conductivity behind its front. When the discharge current reaches its maximum value at $t_1 = 420$ ns, maximum current density is realized at $r \cong 150\ \mu$m and the temperature of the central part of the wire remains rather small. In spite of the fact that in this location the conductivity is ~10 times lower than the normal conductivity, the total resistance of the wire is significantly lower than in the case of the "long" wire explosion. At the time of the maximal amplitude of the resistive voltage ($t_2 \approx 600$ ns, in this case it approximately coincides with t_3), the temperature in the central part of the wire increases and becomes larger than its value at the periphery of the wire. At that time, the value of the total resistance of the wire becomes comparable with the maximal value of the resistance in the case of the "long" wire explosion. Let us note here that at that time (t_2, $t_3 \approx 600$ ns) one obtains a change in the slope of the wire's resistance (see Fig. 7(b)). In addition, at that time the absolute value of the discharge current decreases ~1.4 times as compared with its maximal value. This leads to a ~1.5-fold smaller energy deposition during time $\Delta t = t_2 - t_1$ than in the case of the "long" wire explosion during the corresponding time period. Continuing energy deposition, accompanied by the radial wire expansion, results in a further decrease in its conductivity. Indeed, MHD simulations showed that at $t \approx 960$ ns ($= t_4$) when the wire's resistance reaches its maximal value, the radius of the wire increases ~2 times and the conductivity decreases ~6 times as compared with their value at $t_2 \approx 600$ ns. This leads to a 1.5 times increase in the wire's total resistance. In order to fit this increase in the resistance ($600\ \text{ns} < t < 960\ \text{ns}$), similar to the case of the "long" wire explosion, a new wave of conductivity propagating from the periphery (at $t_2 = 600$ ns) toward the axis was modeled. The comparison between the results of this simplified model and those of the MHD simulations for the "short" wire explosion (see Fig. 7(b)) showed satisfactory agreement.

IV. SUMMARY

To conclude, the results of MHD modeling showed that in order to achieve an optimal electrical explosion of the wire, the temperature and conductivity radial distributions should be uniform across the cross section of the wire at the time when the discharge current reaches its maximal amplitude. The temporal dependence of the total resistance, which dictates the energy deposition rate into the exploding wire, can be obtained using a simplified model of a conductivity wave. Namely, the time when the first conductivity wave approaches the wire's axis and when one obtains the maximal wire's resistance should be close to the time of the maximal current amplitude and resistive voltage. Finally, we want to point out that in the case of extreme high current densities, a simple scaling from a single wire to a wire array having the same total cross-sectional area of wires can lead to a non-optimal wire explosion.

ACKNOWLEDGMENTS

This research was supported by the Israeli Science Foundation Grant No. 99/12.

[1]Ya. E. Krasik, S. Efimov, D. Sheftman, A. Fedotov-Gefen, O. Antonov, D. Shafer, D. Yanuka, M. Nitishinskiy, M. Kozlov, L. Gilburd, G. Toker, S. Gleizer, E. Zvulun, V. Tz. Gurovich, D. Varentsov, and M. Rodionova, IEEE Trans. Plasma Sci. **44**, 412 (2016).
[2]V. Ts. Gurovich, A. Grinenko, Ya. E. Krasik, and J. Felsteiner, Phys. Rev. E **69**, 036402 (2004).
[3]I. V. Oreshkin, R. B. Baksht, A. Yu. Labezkii, A. G. Rousskikh, A. V. Shishlov, P. R. Levashov, K. V. Khishchenko, and I. V. Glazyrin, Tech. Phys. **49**, 843 (2004).
[4]L. I. Chemezova, G. A. Mesyats, V. S. Sedoi, B. N. Semin, and V. V. Valevich, in *18th International Symposium on Discharges and Electrical Insulation in Vacuum, Eindhove* (IEEE, 1998), pp. 48–51.
[5]A. Grinenko, V. Tz. Gurovich, A. Saypin, S. Efimov, and Ya. E. Krasik, Phys. Rev. E **72**, 066401 (2005).
[6]See National Technical Information Service Document No. DE85014241 (S. P. Lyon and J. D. Johnson, Sesame: The Los Alamos National Laboratory Equation-of-State Database, LANL Rep. LA UR-92-3407, 1992). Copies may be ordered from the National Technical Information Service, Springfield, VA, 22161.
[7]Yu. D. Bakulin, V. F. Kuropatenko, and A. V. Luchinskii, Sov. Phys.-Tech. Phys. **21**, 1144–1150 (1976).
[8]A. Grinenko, Ya. E. Krasik, S. Efimov, A. Fedotov, V. Tz. Gurovich, and V. I. Oreshkin, Phys. Plasmas **13**, 042701 (2006).